Inorg. Chem. **2002**, *41*, 4708–4714

The Effect of Ligand Charge on the Coordination Geometry of an Fe(III) Ion: Five- and Six-Coordinate Fe(III) Complexes of Tris(2-benzimidazolylmethyl)amine

Dohyun Moon and Myoung Soo Lah*

Department of Chemistry, College of Science and Technology, Hanyang University, 1271 Sa-1-dong, Ansan, Kyunggi-do 425-170, Korea

Rico E. Del Sesto and Joel S. Miller

Department of Chemistry, University of Utah, 315 S. 1400 E. Salt Lake City, Utah 84112-0850

Received November 12, 2001

By using the tripodal tetradentate ligand tris(2-benzimidazolylmethyl)amine (H_3ntb), which can have several charge states depending on the number of secondary amine protons, mononuclear octahedral and dinuclear trigonal bipyramidal Fe(III) complexes were prepared. The reaction of mononuclear octahedral $[Fe^{III}(H_3ntb)Cl_2]ClO_4$, **1**, with 3 equiv of *sec*-butylamine in methanol led to the formation of mononuclear *cis*-dimethoxo octahedral $Fe^{III}(H_2ntb)(OMe)_2$, **2**. One equivalent of the *sec*-butylamine was used to generate the monoanionic H_2ntb^- ligand where one of the three amines in the benzimidazolyl groups was deprotonated. The remaining 2 equiv were used to generate two methoxides that were coordinated to the octahedral Fe(III) ion in a cis fashion as demonstrated by the chlorides in **1**. Reaction of **1** with excess (7 equiv) *sec*-butylamine generated the doubly deprotonated dianionic $Hntb^{2-}$ that stabilized the dinuclear μ-oxo $Fe^{III}_2O(Hntb)_2$, **3**, adopting a five-coordinate trigonal bipyramidal geometry. The magnetic data for **3** are consistent with the antiferromagnetically coupled Fe^{III} ($S = {}^5/_2$) sites with the coupling constant $J = -127$ cm^{-1}.

Introduction

Model systems that mimic the active sites of metalloenzymes are important not only for the understanding of enzyme mechanisms, but also for the development of small molecular weight biomimetic catalysts. Superoxide dismutases (SOD) are metalloenzymes that disproportionate superoxide into molecular oxygen and hydrogen peroxide through a cyclic oxidation−reduction mechanism.[1] The active site structures of the Mn- and Fe-SODs have a distorted trigonal bipyramidal geometry in both the oxidized and the reduced resting states.[2] It has been proposed that the coordination number of the active sites changes from five-coordinate in the resting states to six-coordinate in both the oxidized and the reduced intermediate states.[2,3] The change in coordination number and geometry was accompanied by a change in charge at the active site through deprotonation of the coordinated water and protonation of the coordinated hydroxide and through the oxidation and reduction of the metal center. Metal complexes possessing ligands capable of being in multiple charge states might yield useful information regarding the relationship between the charge of the ligand and coordination geometry. Recently, we reported a mononuclear octahedral Fe(III) complex containing the tripodal tetradentate ligand tris(2-benzimidazolylmethyl)amine (H_3ntb), in which all three amines of the benzimidazolyl groups are protonated.[4] The ligand may have different charges depending on the number of deprotonated secondary amine groups present (Scheme 1). In this study, we deprotonated the amine protons using *sec*-butylamine to generate negatively charged ligands. We synthesized and

* Author to whom correspondence should be addressed. E-mail: mslah@hanyang.ac.kr.

(1) (a) Fridovich, I. *Annu. Rev. Biochem.* **1995**, *64*, 97−112. (b) Fridovich, I. J. *Biol. Chem.* **1989**, *264*, 7761−7764.
(2) Lah, M. S.; Dixon, M. M.; Pattridge, K. A.; Stallings, W. C.; Fee, J. A.; Ludwig, M. L. *Biochemistry* **1995**, *34*, 1646−1660.
(3) Tierney, D. L.; Fee, J. A.; Ludwig, M. L.; Penner-Hahn, J. E. *Biochemistry* **1995**, *34*, 1661−1668.
(4) Kwak, B.; Cho, K. W.; Pyo, M.; Lah, M. S. *Inorg. Chim. Acta* **1999**, *290*, 21−27.

10.1021/ic011155q CCC: $22.00
Published on Web 08/09/2002

Scheme 1

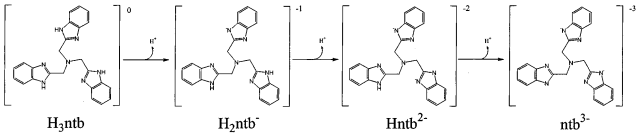

characterized a mononuclear *cis*-dimethoxo octahedral Fe(III) complex containing a singly deprotonated monoanionic ligand, H_2ntb^-, and a dinuclear μ-oxo trigonal bipyramidal Fe(III) complex containing a doubly deprotonated dianionic ligand, $Hntb^{2-}$.

Experimental Section

Materials. The following were used as received with no further purification: *sec*-butylamine from Aldrich Inc., and methanol from Carlo Erba. $[Fe^{III}(H_3ntb)Cl_2]ClO_4$, **1**, was prepared according to literature procedure.[4]

Instrumentation. C, H, N,and Fe determinations were performed by the Elemental Analysis Laboratory of the Korean Institute of Basic Science. Infrared spectra were recorded in the 4000−600 cm^{-1} range on a Bio-Rad ATR FT-IR spectrometer.

Synthesis: $Fe^{III}(H_2ntb)(OMe)_2$, 2. To **1** (0.31 g, 0.50 mmol) dissolved in 20 mL of methanol was added *sec*-butylamine (0.15 mL, 1.5 mmol). The solution was stirred for 2 min and filtered, and the filtrate was allowed to stand for 5 days, after which time pale red crystals (0.22 g, 81% yield) formed. Elemental analysis suggested that when exposed to air, solvent methanol within the crystal was replaced by water. Anal. Calcd for $Fe^{III}(H_2ntb)(OMe)_2 \cdot H_2O$ ($FeC_{26}H_{28}N_7O_3$) (fw 542.40): C, 57.57; H, 5.20; N, 18.08; Fe, 10.30. Found: C, 57.6; H, 5.35; N, 17.7; Fe, 10.8. μ_{eff}: 5.68 μ_B.

$Fe^{III}_2O(Hntb)_2$, 3. To **1** (0.31 g, 0.50 mmol) dissolved in 20 mL of methanol was added *sec*-butylamine (0.35 mL, 3.5 mmol). The solution was stirred for 2 min and filtered, and the filtrate was allowed to slowly evaporate for 2 days, after which time red crystals (0.17 g, 67% yield) formed. Elemental analysis suggested that when exposed to air, solvent methanol within the crystal was replaced by water. Anal. Calcd for $Fe^{III}_2O(Hntb)_2 \cdot 4H_2O$ ($Fe_2C_{48}H_{46}N_{14}O_5$) (fw 1010.68): C, 57.04; H, 4.59; N, 19.40; Fe, 11.05. Found: C, 56.80; H, 4.48; N, 19.37; Fe, 10.8. IR 834 cm^{-1} (for $Fe-O-Fe_{asym}$).

Magnetic Measurement. Room-temperature magnetic susceptibilities of well-ground solid samples were measured by the Gouy method. All measurements were calibrated against a $Hg[Co(SCN)_4]$ standard. Temperature-dependent magnetic susceptibility measurements were carried out on powdered samples between 2 and 300 K, using a Quantum Design MPMS-5XL SQUID ac/dc magnetometer.[5] Samples were cooled in zero field and the data were collected in a 1000 G field upon warming. The diamagnetic correction for **3** (-598×10^{-6} emu mol^{-1}) was calculated from Pascal's constants.[6]

X-ray Crystallography. Crystals mounted on glass fiber were studied with a Siemens SMART CCD Detector single-crystal X-ray diffractometer with a graphite monochromated Mo Kα radiation ($\lambda = 0.71073$ Å) source equipped with a sealed tube X-ray source at −100 °C. Preliminary unit cell constants were determined with a set of 45 narrow frame (0.3° in ω) scans. A data sets consisted of 1286 frames of intensity data collected with a frame width of 0.3° in ω, a counting time of 25 s/frame, and a crystal-to-detector distance of 5.0 cm. The double pass method of scanning was used to exclude any noise. The collected frames were integrated by using an orientation matrix determined from the narrow frame scans. SMART and SAINT software packages[7] were used for data collection and data integration. Analysis of the integrated data did not reveal any decay. Final cell constants were determined by a global refinement of 8192 reflections ($\theta < 25.0°$). Collected data were corrected for absorbance by using SADABS[8] based upon the Laue symmetry using equivalent reflections. Structure solution and refinement were carried out with the SHELXTL-PLUS software package[9] and the structure solved by the direct method. Full-matrix least-squares refinement was carried out by minimizing $(F_o^2 - F_c^2)^2$. All non-hydrogen atoms were refined anisotropically; hydrogen atoms were located and refined isotropically or assigned isotropic displacement coefficients $U(H) = 1.2U(C)$ or $1.5U$(C-methyl), and their coordinates were allowed to ride on their respective atoms.

$Fe(H_2ntb)(OMe)_2 \cdot 3MeOH$, 2. Two solvent molecules coordinated to the metal ion were treated as methoxides. Three additional methanol sites were identified but two of these were statistically disordered.

$Fe_2O(Hntb)_2 \cdot 10MeOH$, 3. Five methanol sites were identified, but two of these were partially occupied and one was statistically disordered.

Crystal data and intensity data collection parameters are listed in Table 1.

Results and Discussion

The reaction of $[Fe(H_3ntb)Cl_2]ClO_4$, **1**, with various weak bases (potassium superoxide, sodium acetate, hexamethylene diamine) led to the formation of the dinuclear octahedral Fe(III) complex, $[Fe_2O(H_3ntb)_2Cl_2](ClO_4)_2$ (Scheme 2).[4,14a] The Fe(III) center in the dinuclear complex maintained the same octahedral geometry as in **1**. The chloride trans to the benzimidazole group was substituted with a bridging oxo oxygen to form a μ-oxo-bridged dinuclear complex, in which the ligand is fully protonated and neutral. The secondary amine sites on H_3ntb can be deprotonated to yield various

(5) Brandon, E. J.; Rittenberg, D. K.; Arif, A. M.; Miller, J. S. *Inorg. Chem.* **1998**, *37*, 3376−3384.
(6) O'Connor, C. J. *Prog. Inorg. Chem.* **1982**, *29*, 203−283.
(7) *SMART* and *SAINT*, Area Detector Software Package and SAX Area detector Integration Program; Bruker Analytical X-ray: Madison, WI, 1997.
(8) *SADABS*, Area Detector Absorption Correction Program; Bruker Analytical X-ray: Madison, WI, 1997.
(9) Sheldrick, G. M. *SHELXTL-PLUS*, Crystal Structure Analysis Package; Bruker Analytical X-ray: Madison, WI, 1997.
(10) (a) Kurtz, D., Jr. *Chem. Rev.* **1990**, *90*, 585−606. (b) Junk, P. C.; McCool, B. J.; Moubaraki, B.; Murray, K. S.; Spiccia, L. *Angew. Chem., Int. Ed. Engl.* **1999**, *38*, 2224−2226.
(11) (a) Roelfes, G.; Lubben, M.; Chen, K.; Ho, R. Y. N.; Meetsma, A.; Genseberger, S.; Hermant, R. M.; Hage, R.; Mandal, S. K.; Young, V. G., Jr.; Zang, Y.; Kooijman, H.; Spek, A. L.; Que, L., Jr.; Feringa, B. L. *Inorg. Chem.* **1999**, *38*, 1929−1936. (b) Jonas, R. T.; Stack, T. D. P. *J. Am. Chem. Soc.* **1997**, *119*, 8566−8567. (c) Lecomte, C.; Chadwick, D. L.; Coppens, P.; Stevens, E. D. *Inorg. Chem.* **1983**, *22*, 2982−2992. (d) Belle, C.; Gautier-Luneau, I.; Pierre, J.-L.; Scheer, C.; Saint-Aman, E. *Inorg. Chem.* **1996**, *35*, 3706−3708. (e) Hoard, J. L.; Hamor, M. J.; Harmor, T. A.; Cauughey, W. S. *J. Am. Chem. Soc.* **1965**, *87*, 2312−2319. (f) Hatano, K.; Uno, T. *Bull. Chem. Soc. Jpn.* **1990**, *63*, 1825−1827. (g) Holman, T. R.; Andersen, K. A.; Anderson, O. P.; Hendrich, M. P.; Juarez-Garcia, C.; Münck, E.; Que, L., Jr. *Angew. Chem., Int. Ed.* **1990**, *29*, 921−923. (h) Johnson, M. R.; Seok, W. K.; Ma, W.; Slebodnick, C.; Wilcoxen, K. M.; Ibers, J. A. *J. Org. Chem.* **1996**, *61*, 3298−3303. (i) Prévot, L.; Jaquinod, L.; Fischer, J.; Weiss, R. *Inorg. Chim. Acta* **1998**, *283*, 98−104. (j) Taft, K. L.; Caneschi, A.; Pence, L. E.; Delfs, C. D.; Papaefthymiou, G. C.; Lippard, S. J. *J. Am. Chem. Soc.* **1993**, *115*, 11753−11766.
(12) Than, R.; Schrodt, A.; Westerheide, L.; van Eldik, R.; Krebs, B. *Eur. J. Inorg. Chem.* **1999**, 1537−1543.

Table 1. Crystal Data and Structure Refinement for **2** and **3**

	2	**3**
formula	$C_{29}H_{38}FeN_7O_5$	$C_{29}H_{39}FeN_7O_{5.5}$
fw	620.51	629.52
cryst system, space group	monoclinic, $P2_1/c$ (no. 14)	triclinic, $P\bar{1}$ (no. 2)
unit cell dimens (Å, deg)	$a = 11.541(3)$	$a = 12.1896(5)$, $\alpha = 99.328(1)$
	$b = 21.621(6)$, $\beta = 110.437(5)$	$b = 12.5237(5)$, $\beta = 109.334(1)$
	$c = 13.192(4)$	$c = 12.9989(5)$, $\gamma = 118.218(1)$
V (Å^3)	3084.7(16)	1523.99(11)
Z, calcd density (mg/m^3)	4, 1.336	2, 1.372
abs coeff (mm^{-1})	0.538	0.546
cryst size (mm^3)	0.50 × 0.25 × 0.14	0.50 × 0.35 × 0.15
θ range for data collcn (deg)	1.88 to 28.32	1.80 to 28.31
reflcns collcd/unique	18837/7351 [R(int) = 0.0260]	9846/6893 [R(int) = 0.0189]
goodness-of-fit on F^2	1.143	1.045
final R indices [$I > 2\sigma(I)$]	R1[a] = 0.0618, wR2[b] = 0.1639	R1 = 0.0472, wR2 = 0.1341
R indices (all data)	R1 = 0.0703, wR2 = 0.1676	R1 = 0.0520, wR2 = 0.1391
largest diff peak and hole (e Å^{-3})	0.753 and −0.686	0.627 and −0.678

[a] $R1 = \sum||F_o| - |F_c||/\sum|F_o|$. [b] $wR2 = [\sum w(F_o^2 - F_c^2)^2/\sum wF_o^4]^{1/2}$.

Scheme 2

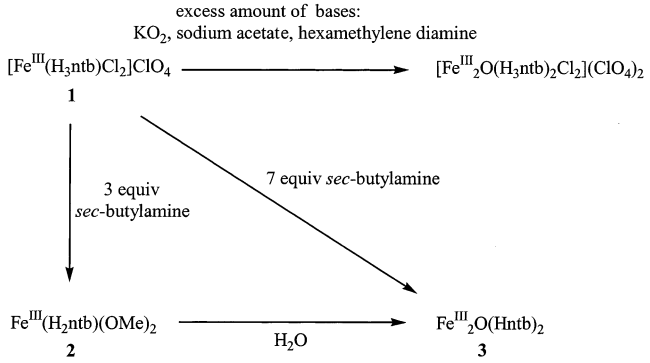

deprotonated forms with their corresponding charges. Herein, we report on the products isolated when 3 and 7 equivalents of *sec*-butylamine are added to **1**. Reaction of **1** with 3 equivalents of *sec*-butylamine in methanol leads to the formation of the mononuclear octahedral complex $Fe(H_2ntb)(OMe)_2$, **2**, where one of the amine groups of the ligand is deprotonated to serve as the monoanionic H_2ntb^-. The base was also used to generate two methoxides that are coordinated to the octahedral Fe(III) ion. On the other hand, reaction of **1** with 7 equiv of *sec*-butylamine in methanol forms the μ-oxo dinuclear trigonal bipyramidal complex $Fe_2O(Hntb)_2$, **3**, where two of the amine groups of the ligand are deprotonated to serve as the dianionic $Hntb^{2-}$. This result contrasts with the conversion of mononuclear octahedral Fe(III) complex **1** to the dinuclear octahedral Fe(III) complex $[Fe_2O(H_3ntb)_2Cl_2](ClO_4)_2$ with use of excess amounts of weak bases. Here, the bases are only used to generate the μ-oxo bridge, and the ligand remains in the neutral H_3ntb form (Scheme 2).[4]

The room-temperature magnetic moment of **2** is 5.68 μ_B, which is comparable to the spin-only value of high-spin d^5 Fe^{III} (5.92 μ_B). Exposure of a solution of **2** to air resulted in the slow formation of a new complex that displayed an additional characteristic band at 834 cm^{-1}. This band, assigned as an Fe−O−Fe asymmetric stretch, has been observed in the other oxo-bridged dinuclear ferric complexes.[10] The IR spectrum of this new complex is identical with that of **3**. Addition of a drop of water into the solution facilitated the conversion of **2** to **3**. Formation of the oxo ligand from water in **3** was confirmed by labeling studies. The Fe−^{16}O−Fe asymmetric stretching band at 834 cm^{-1} in the IR spectrum of **3** shifts to 799 cm^{-1} in ^{18}O-labeled **3**.

Molecular Structure of $Fe(H_2ntb)(OMe)_2$, 2. The tetradentate H_2ntb^- ligand occupies four of the six Fe octahedral coordination sites, with the OMe group occupying the remaining two cis positions (Figure 1). The overall geometry of **2** is very similar to that of reactant **1** (Table 2). In **1**, H_3ntb is a neutral ligand with all the amines of the benzimidazolyl groups being fully protonated and **1** is a monocationic complex ion. In **2**, however, H_2ntb^- is a monoanionic ligand where one of the amines of the benzimidazolyl groups is deprotonated and **2** is a neutral complex. The deprotonated amine (N3) of the benzimidazolyl group in **2** serves as a hydrogen bond acceptor, while the protonated amines (N5 and N7) serve as hydrogen bond donors (Table 3). The bond distance between the Fe(III) ion and the tertiary apical nitrogen atom (N1) of 2.397 Å is about 0.29 Å longer

(13) (a) Watton, S. P.; Masschelein, A.; Rebek, J., Jr.; Lippard, S. J. *J. Am. Chem. Soc.* **1994**, *116*, 5196−5205. (b) Lynch, V. M.; Sibert, J. W.; Sessler, J. L.; Davis, B. E. *Acta Crystallogr.* **1991**, *C47*, 866−869. (c) Lah, M. S.; Kirk, M. L.; Hatfield, W.; Pecoraro, V. L. *J. Chem. Soc., Chem. Commun.* **1989**, 1606−1608. (d) Fallon, G. D.; Markiewicz, A.; Murray, K. S.; Quach, T. *J. Chem. Soc., Chem. Commun.* **1991**, 198−200. (e) Degang, F.; Guoxiong, W.; Wenxiz, T.; Kaibei, Y. *Polyhedron* **1993**, *12*, 2459−2463. (f) Ainscough, E. W.; Brodie, A. M.; Plowman, J. E.; Brown, K. L.; Addison, A. W.; Gainsford, A. R. *Inorg. Chem.* **1980**, *19*, 3655−3663. (g) Asirvatham, S.; Khan, M. A.; Nicholas, K. M. *Inorg. Chem.* **2000**, *39*, 2006−2007. (h) Taft, K. L.; Masschelein, A.; Liu, S.; Lippard, S. J.; Garfinkel-Shweky, D.; Bino, A. *Inorg. Chim. Acta* **1992**, *198−200*, 627−631. (i) Re, N.; Crescenzi, R.; Floriani, C.; Miyasaka, H.; Matsumoto, N. *Inorg. Chem.* **1998**, *37*, 2717−2722. (j) Healy, P. C.; Patrick, J. M.; Skelton, B. W.; White, A. H. *Aust. J. Chem.* **1983**, *36*, 2031−2041. (k) Lloret, F.; Julve, M.; Faus, J.; Solans, X.; Journaux, Y.; Morgenstern-Badarau, I. *Inorg. Chem.* **1990**, *29*, 2232−2237. (l) Senge, M. O. *Acta Crystallogr.* **1996**, *C52*, 302−305. (m) Aruffo, A. A.; Murphy, T. B.; Johnson, D. K.; Rose, N. J.; Schomaker, V. *Inorg. Chim. Acta* **1982**, *67*, L25−L27. (n) Eulering, B.; Schmidt, M.; Pinkernell, U.; Karst, U.; Krebs, B. *Angew. Chem., Int. Ed.* **1996**, *35*, 1973−1974.

(14) (a) Buchanan, R. M.; O'Brien, R. J.; Richardson, J. F.; Latour, J.-M. *Inorg. Chim. Acta* **1993**, *214*, 33−40. (b) Kwak, B.; Lah, M. S. *Bull. Korean Chem. Soc.* **2000**, *21*, 65−68. (c) Payra, P.; Hung, S.-C.; Kwok, W. H.; Johnston, D.; Gallucci, J.; Chan, M. K. *Inorg. Chem.* **2001**, *40*, 4036−4039. (d) Li, A.-R.; Wei, H.-H.; Gang, L.-L. *Inorg. Chim. Acta* **1999**, *290*, 51−56. (e) Calderazzo, F.; Labella, L.; Marchetti, F. *J. Chem. Soc., Dalton Trans.* **1998**, 1485−1489.

Table 2. Selected Bond Lengths (Å) and Angles (°) for **1**[a], **2** and **3**

1		**2**		**3**	
		distances			
Fe1−N1	2.332(6)	Fe1−N1	2.397(3)	Fe1−N1	2.383(2)
Fe1−N2	2.091(6)	Fe1−N2	2.077(3)	Fe1−N2	2.010(2)
Fe1−N4	2.095(6)	Fe1−N4	2.106(3)	Fe1−N4	1.996(2)
Fe1−N6	2.131(6)	Fe1−N6	2.131(3)	Fe1−N6	2.064(2)
Fe1−Cl1	2.214(3)	Fe1−O1	1.861(3)	Fe1−O1	1.7886(3)
Fe1−Cl2	2.348(3)	Fe1−O2	1.992(2)		
		angles			
N1−Fe1−N2	74.8(2)	N2−Fe1−N1	74.40(10)	N2−Fe1−N1	75.87(7)
N1−Fe1−N4	74.6(2)	N4−Fe1−N1	73.91(10)	N4−Fe1−N1	75.52(6)
N1−Fe1−N6	77.6(2)	N6−Fe1−N1	76.45(10)	N6−Fe1−N1	74.67(6)
N1−Fe1−Cl1	174.5(2)	O1−Fe1−N1	172.72(10)	O1−Fe1−N1	178.50(4)
N2−Fe1−N4	149.4(2)	N2−Fe1−N4	148.27(11)	N2−Fe1−N4	114.94(7)
N2−Fe1−N6	86.9(2)	N2−Fe1−N6	86.09(11)	N2−Fe1−N6	113.34(7)
N4−Fe1−N6	86.8(2)	N4−Fe1−N6	84.90(11)	N4−Fe1−N6	113.23(7)
				Fe1−O1−Fe1[b]	180.0

[a] Reference 4. [b] Inversion symmetry related atom.

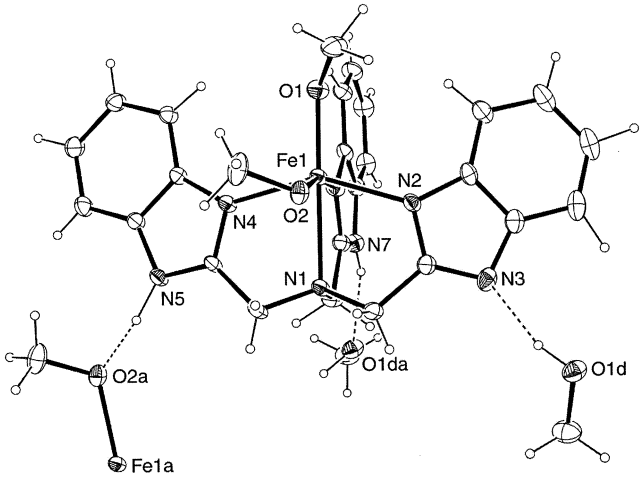

Figure 1. ORTEP drawing (30%) of $Fe^{III}(H_2ntb)(OMe)_2$, **2**. One among three amine protons of the benzimidazolyl groups was deprotonated and the ligand served as the monoanionic H_2ntb^-. While N5 and N7 of the neutral benzimidazole groups serve as hydrogen donors, N3 of the anionic benzimidazolate group serves as a hydrogen acceptor.

Table 3. Hydrogen Bonds (Å and deg) in the Crystal Structures of **2** and **3**

D−H···A	*d*(D−H)	*d*(H···A)	*d*(D···A)	∠(DHA)
		2		
O1D−H1D···N3	0.97(7)	1.82(7)	2.763(4)	163(6)
O3D−H3D1···O2D	0.83	2.53	2.93(5)	111.2
O32D−H32D···O22D	0.83	2.46	2.95(5)	118.6
N5−H5N5···O2[a]	1.07(6)	1.49(6)	2.547(4)	173(5)
N7−H7N7···O1D[a]	0.81(4)	1.99(4)	2.766(4)	159(4)
O22D−H22D···O22D[b]	1.02	1.66	2.62(6)	155.8
		3		
N7−H1N7···O2[c]	0.83(3)	1.87(3)	2.692(3)	175(3)
O2−H1O2···N5	0.89(4)	1.81(4)	2.686(3)	172(3)
O3−H1O3[d]···N3	0.82(4)	1.93(4)	2.712(3)	158(4)
O4−H1O4···O5[e]	0.77(6)	1.83(6)	2.558(6)	156(7)
O4−H1O4···O7[f]	0.77(6)	2.41(7)	3.095(14)	149(7)
O5−H1O5···O6[g]	0.82	1.99	2.635(7)	134.6
O6−H1O6···O3	0.82	1.81	2.620(6)	167.1

[a] [−g]Symmetry transformations used to generate equivalent atoms: (*a*) *x*, $-y + 3/2$, $z + 1/2$; (*b*) $-x$, $-y + 1$, $-z$; (*c*) $-x + 1$, $-y + 1$, $-z + 2$; (*d*) $x + 1$, *y*, $z + 1$; (*e*) $-x + 1$, $-y + 1$, $-z + 1$; (*f*) $-x$, $-y + 1$, $-z + 1$; (*g*) $x + 1$, *y*, *z*.

than those between the Fe(III) ion and the basal nitrogen atoms of the benzimidazolyl groups (av 2.105 Å). The Fe−O bond length trans to the basal benzimidazolyl nitrogen atom (Fe1−O2: 1.992 Å) is about 0.13 Å longer than the Fe−O bond length trans to the apical tertiary nitrogen atom (Fe1−O1: 1.867 Å) (Table 2). A similar trend was observed in the *cis*-dichloro complex **1**. The Fe−Cl bond length trans to the basal benzimidazolyl nitrogen atom (Fe1−Cl2: 2.348 Å) is also about 0.13 Å longer than the Fe−Cl bond length trans to the apical tertiary nitrogen atom (Fe1−Cl1: 2.214 Å). The length of the Fe(III)−O bond where the oxygen is situated trans to the apical tertiary nitrogen atom falls within the range of lengths previously determined for terminally bound methoxides in structurally characterized Fe(III) complexes (Table 4).[11] However, the length of the Fe(III)−O bond where the oxygen is situated trans to the neutral basal benzimidazolyl nitrogen atom is longer than those previously determined for terminally bound methoxides, but is shorter than those for terminally bound methanols (Table 4).[11−13] Although the Fe1−O2 bond length is marginally longer than that expected for a methoxide, based on a similar elongation of the basal bond length in *cis*-dichloro complex **1**, and the absence of any counterions, O2 was assigned as the oxygen atom of the methoxide.

Molecular Structure of $Fe_2O(Hntb)_2$, 3. 3 is a dinuclear μ-oxo Fe(III) complex where the bridging oxo atom is at the crystallographic inversion center and belongs to the pseudo-D_{3d} point group (Figure 2). The metal center has trigonal bipyramidal geometry (Figure 2a and Table 2). The three nitrogen atoms of benzimidazole groups form the base of the trigonal bipyramidal geometry. The apical nitrogen atom of $Hntb^{2-}$ occupies one axial site, while a bridging oxygen atom occupies the other. The length of the Fe(III)−oxo oxygen atom bond (1.7886(3) Å) in **3** is approximately the same as those lengths previously determined in other similar oxo-bridged dinuclear Fe(III) complexes.[10,14] While the ligand serves as a neutral H_3ntb ligand in **1**, and as a monoanionic H_2ntb^- ligand in **2**, it is a dianionic $Hntb^{2-}$ ligand in **3** where two of three amine groups are deprotonated. The deprotonated N3 and N5 atoms again serve as hydrogen bond acceptors while the protonated N7 atom serves as a hydrogen bond donor (Table 3). The bond distance between the Fe(III) ion and the tertiary apical

Table 4. Comparison of Bond Lengths (Å) between the Fe^{III}-Terminal Methoxy Bond and the Fe^{III}-Terminal Methanol Bond[aa]

Fe^{III}-terminal methoxy bond	
$[(N4Py)Fe(OMe)]^{2+}$ [a]	1.772
$[(PY5)Fe(OMe)]^{2+}$ [b]	1.782(3)
$[(N4Py)Fe(OMe)]^{2+}$ [a]	1.789
$[(TPP)FeOMe]^{+}$ [c]	1.816(2)
$[(L)Fe_2(\mu\text{-OMe})(OMe)]^{+}$ [d]	1.830
[(meso-DME)Fe(OMe)][e]	1.842(4)
[(OEP)Fe(OMe)][f]	1.843(2)
$[(bpmp)CuFe\ (O_2CCH_3)(OMe)]^{2+}$ [g]	1.849(4)
[(capped-Por)Fe(OMe)][h]	1.851
complex **2**	**1.861(3)**; apical Fe^{III}−O distance
[(strapped-Por)Fe(OMe)][i]	1.867(3)
$[Fe_4(OMe)_5(MeOH)_3(OBz)]$[j]	1.94(5)
complex **2**	**1.992(2)**; basal Fe^{III}−O distance
$Fe^{III}{}_2$-terminal methanol−methoxy bond[z]	
$[(tbpo)Fe_2(O_2As(CH_3)_2)(MeO{-}H{-}OMe)]$[k]	1.993(3), 1.997(3)
Fe^{III} -terminal methanol bond	
$[(xdk)Fe_2O(MeOH)_5(H_2O)]^{2+}$ [l]	2.083(7), 2.070(8), 2.082(7), 2.07(1)
$[Fe_3(\mu 3\text{-O})(OBz)_6(MeOH)_2(H_2O)]^{+}$ [m]	2.080(4), 2.077(4)
$[Fe_4(shi)_3(OAc)_3(MeOH)_3]$[n]	2.08(1)
$[Fe_2(bsdp)(OMe)Cl_2(MeOH)]$[o]	2.085(2)
$[Fe_3(\mu^3\text{-O})(OBz)_6(MeOH)_3]^{+}$ [p]	2.084(5), 2.095(5), 2.090(5)
$[Fe(mpp)_2(MeOH)_2]^{+}$ [q]	2.094(3)
$[Fe_{10}Cl_8O_4(OMe)_{14}(MeOH)_6]$[r]	2.131(2) 2.102, 2.086
$[Fe_2O(BIPhMe)_2(O_2CCH_3)(MeOH)_2]^{+}$ [s]	2.103(5), 2.118(5)
$[Fe(salen)(MeOH)_2]^{+}$ [t]	2.12(1), 2.12(1)
$[Fe(phen)Cl_3(MeOH)]$[u]	2.136(5)
$[Fe_2(\mu\text{-sq})(salen)_2(MeOH)_2]$[v]	2.158(4)
$[Fe(OEP)(MeOH)]^{+}$ [w]	2.159(3)
$[FeCl_2(sbh)(MeOH)]$[x]	2.171(3)
$[Fe(mtbpo)Cl_2(O_2As(CH_3)_2)(MeOH)]^{2+}$ [y]	2.247(3)

[a−j] References 11a−11j. [k] Reference 12. [l−y] References 13a−13n. [z] A methanol and a methoxy group together behaved as a monoanionic bidentate ligand $[MeO\cdots H\cdots OMe]^{-}$ where the proton was assumed to be positioned between the oxygen atoms. [aa] N4PY = *N*,*N*-bis(2-pyridylmethyl)-*N*-(bis-2-pyridylmethyl)amine; PY5 = 2,6-bis((2-pyridyl)methoxymethane)pyridine; TPP = tetraphenylporphyrin dianion; L = 2-(bis(2′-hydroxyphenyl)amino)methyl-6-(bis(2″-pyridylmethyl)amino)methyl-4-methylphenolate; meso-DME = mesoporphyrin-IX dimethyl ester dianion; OEP = octaethylporphyrin dianion; bpmp = 2,6-bis((bis(2-pyridylmethyl)amino)methyl)-4-methylphenolate; capped-Por = 1,2,4,5-tetrahydroxybenzene-cpped tetra(*o*-ethoxyphenyl)porphyrin dianion; strapped-Por = 5,15-(*o*,*o*′-(2-methyl-2′-hydroxy-3,3′-diamidobiphenyl)diphenyl)porphyrin; OBz = benzoate; tbpo = *N*,*N*,*N*′,*N*′-tetrakis(2-benzimidazolylmethyl)-1,3-diamino-2-propanolate; xdk = *m*-xylenediamine-bis(Kemp's triacid)imide; shi = salicylhydroximate; bsdp = *N*,*N*′-bissalicylidene-1,3-diaminopropan-2-ol; mpp = 2-(5-methylpyrazol-3-yl)phenolate; BIPhMe = bis(1-methylimidazol-2-yl)phenylmethoxymethane; sq = the dianion of 3,4-dihydroxy-3-cyclobutene-1,2-dion; salen = *n*,*n*-ethylenebis(salicyidineiminato) dianion; phen = 1,10-phenanthroline; sbh = salicylaldehyde benzoylhydrazone; mtbpo = *N*-methyl-*N*,*N*′*N*′-tris(2-benzimidazolylmethyl)-2-hydroxy-1,3-diaminopropanolate.

nitrogen atom (N1) of 2.383 Å is approximately 0.36 Å longer than those between the ferric ion and the basal nitrogen atoms of the benzimidazolyl groups (av 2.023 Å). The bond angles around the basal plane (N2−Fe1−N4 114.94(7)°, N2−Fe1−N6 113.34(7)°, N4−Fe1−N6 113.23(7)°) are very close to each other but deviate from the 120° angle expected for a truly trigonal bipyramidal geometry. The deviation is brought about by a 0.5 Å displacement of the Fe(III) ion above the triangular basal plane toward the bridging oxo atom. The bond length of the Fe(III)-anionic benzimidazolate (2.077 Å) in **2** is approximately 0.04 Å shorter than that of the Fe(III)-neutral benzimidazole (av 2.119 Å). The bond length of the Fe(III)-anionic benzimidazolate (2.003 Å) in **3** is again approximately 0.06 Å shorter than that of the Fe(III)-neutral benzimidazole (av 2.064 Å). The anionic benzimidazolates are coordinated to the iron centers more strongly than the neutral benzimidazoles in both complexes. An interesting observation is that the length of the Fe(III)-neutral benzimidazole bond in **3** is shorter than that of the Fe(III)-anionic benzimidazolate bond length in **2**. The overall decrease in bond lengths around the metal center in five-coordinate complex **3** compared to those in six-coordinate complex **2**[15] lead to the shorter Fe(III)-neutral benzimidazole bond length in **3** than the Fe(III)-anionic benzimidazolate bond length in **2**. The bond distance between the Fe(III) ion and the anionic benzimidazolyl nitrogen atom is shorter than those between the Fe(III) ion and the corresponding neutral benzimidazolyl nitrogen atoms (Table 2).

Magnetic Properties. The 2 to 300 K magnetic susceptibility (χ) data for **3** were not amenable to the Curie−Weiss expression. In accordance with the dinuclear structure, χ was modeled by using a Bleaney−Bowers type expression for two interacting $S = {}^5/_2$ Fe^{III} spins:[6]

$$\chi = \left[(1-y)\frac{N\mu_B{}^2 g^2}{k_B(T-\theta)}\frac{2e^{2J/T}+10e^{6J/T}+28e^{12J/T}+60e^{20J/T}+110e^{30J/T}}{1+3e^{2J/T}+5e^{6J/T}+7e^{12J/T}+9e^{20J/T}+11e^{30J/T}}\right] + \left[(y)\frac{N\mu_B{}^2 g^2 S(S+1)}{3k_B(T-\theta)}\right] \quad (1)$$

where N is Avogadro's number, μ_B is the Bohr magneton, g

(15) The average bond length (2.023 Å) of the Fe(III)−imine nitrogen atoms in **3** is approximately 0.08 Å shorter than that found in **2** (2.105 Å). Two factors thought to contribute to a shortening of the bond length are the decrease in coordination number from six to five and the increase in negative charge of the ligand from −1 to −2.

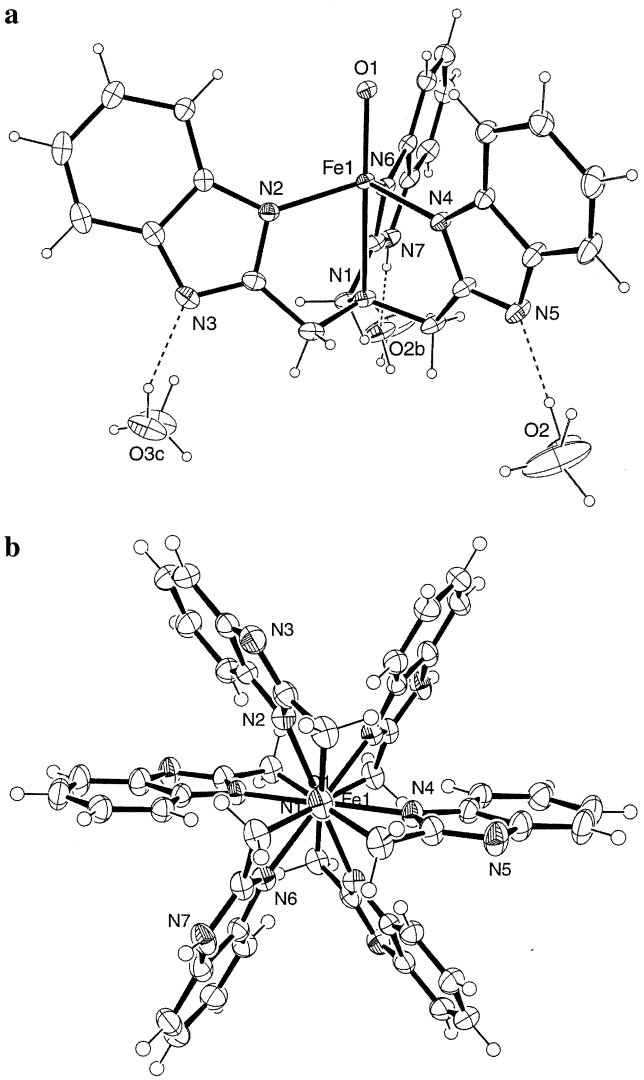

Figure 2. (a) ORTEP drawing (30%) of part of $Fe^{III}_2O(Hntb)_2$, **3**. Two among three amine protons of the benzimidazolyl groups were deprotonated and the ligand served as the dianionic $Hntb^{2-}$. The oxygen atom at the apical position of the trigonal-bipyramidal geometry is in the crystallographic inversion center. While N7 of the neutral benzimidazole group serves as the hydrogen donor, N3 and N5 of the anionic benzimidazolate groups serve as hydrogen acceptors. (b) View along the Fe−O−Fe axis.

is the Lande g-value, k_B is Boltzmann's constant, θ is the Weiss constant for weak intermolecular interactions, and J describes the strong intramolecular interaction between the Fe(III) centers within the dimer. A Curie−Weiss term is added to the Bleaney−Bowers (right-hand side of the equation) term and weighted accordingly to account for monomeric Fe(III) $S = {}^5/_2$ impurities, with y representing the fraction of monomers present in the sample.

The increase in χ at low temperature is attributed to a monomeric $S = {}^5/_2$ impurity, and it is accounted for by the right-hand term in eq 1. The $\chi(T)$ for **3** can be modeled by using eq 1, with $J = -127$ cm^{-1}, $\theta = -3.7$ K, and 2.6% $S = {}^5/_2$ impurity (Figure 3). The g value is assumed to be 2.00 in accordance with a $^6A_{1g}$ ground state for the Fe(III) site. This singlet-undecet splitting is consistent with other strongly coupled oxo-bridged Fe(III) dimers, which range from −42 to −191 cm^{-1}.[10a,14a] The experimental J value for **3** is in the range of values reported for other oxo-bridged Fe^{III}

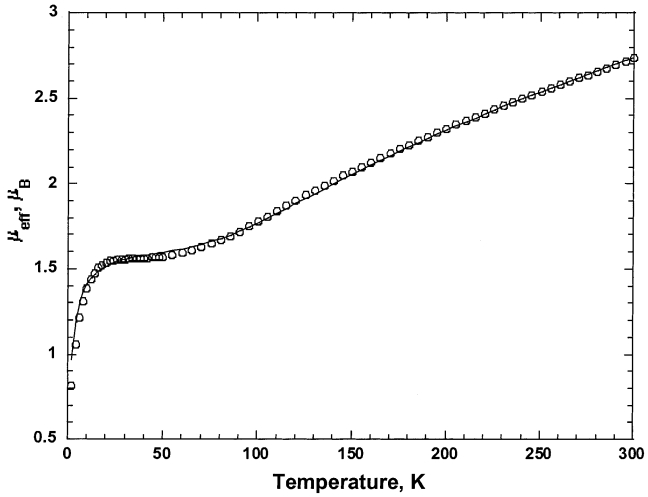

Figure 3. Plot of magnetic moment, μ_{eff}, vs T for **3**. The solid line is the fit of the data to eq 1.

complexes,[10a] but is larger than the reported value of −100 cm^{-1} for the similar octahedral complex $[Fe_2O(H_3ntb)Cl_2](PF_6)_2$ containing the neutral H_3ntb ligand as opposed to the anionic $Hntb^{2-}$ ligand present in **3**.[14a] The difference in J values of 27 cm^{-1} could not be explained by the difference in the bridging bond distances. It is known that the J values in oxo-bridged Fe(III) dimers are correlated to the bridging bond distances.[16a] The Fe−O bond distance in complex **3** is only approximately 0.016 Å shorter than that in $[Fe_2O(H_3ntb)Cl_2](PF_6)_2$. This difference in bond distance accounts for only 8 cm^{-1} in the J value. Considering the uncertainty of less than ∼10 cm^{-1} in the J value for the complex,[17] the remaining 19 cm^{-1} discrepancy in the J values cannot be fully explained by the experimental error. This discrepancy should come from the change of the coordination environment of the ferric center from six-coordinate octahedral geometry to five-coordinate trigonal bipyramidal geometry and/or the change of the ligand charge from neutral H_3ntb ligand to the dianionic $Hntb^{2-}$ ligand.

When 3 equiv of *sec*-butylamine were added to **1**, complex **2**, possessing two methoxide ligands, was obtained. One equivalent of *sec*-butylamine deprotonated one of the three amines of the ligand, while 2 equiv of *sec*-butylamine generated the two methoxides that were coordinated to the octahedral Fe(III) ion in **2**. Although the coordination number in both complexes was the same (six), the overall charge of the complex changed from +1 to 0. When excess (7 equiv) *sec*-butylamine was used as a base, in addition to **1** being converted to the μ-oxo-bridged dinuclear complex, two amine protons of the ligand were deprotonated to generate dianionic $Hntb^{2-}$. The strongly electron donating dianionic $Hntb^{2-}$ with a bridging oxide anion could stabilize a five-coordinate Fe(III) ion. The tripodal nature of the H_3ntb ligand could stabilize the trigonal bipyramidal geometry of the metal ions

(16) (a) Weihe, H.; Güdel, H. U. *J. Am. Chem. Soc.* **1997**, *119*, 6539−6543. (b) Mukherjee, R. N.; Stack, T. D. P.; Holm, R. H. *J. Am. Chem. Soc.* **1988**, *110*, 1850−1861.

(17) It has been suggested that different analyses of the same susceptibility data can lead to J values varying by as much as 21 cm^{-1} when the g value is allowed to float for a ferric center.[16] However, a fixed $g = 2.00$ value gives only an ∼10 cm^{-1} variation in the J values.

with less geometrical preference, such as Mn(II) and Zn(II) ions. Trigonal bipyramidal geometries with neutral H_3ntb ligands were reported for [Mn(II)(H_3ntb)Cl]Cl[18] and isostructural [Zn(II)(*N*-methyl-H_3ntb)Cl]Cl.[19] However, a neutral H_3ntb, or the monoanionic H_2ntb^-, could only stabilize the octahedral Fe(III) complexes. Only a few trigonal bipyramidal Fe(III) complexes are known.[20] **3** is the first μ-oxo-bridged dinuclear Fe(III) complex with local trigonal bipyramidal geometry. The rare trigonal bipyramidal geometry of the Fe(III) complex resulted from the geometrical and charge contribution of the tripodal dianionic $Hntb^{2-}$ ligand. In addition to the trigonal pyramidal nature of the $Hntb^{2-}$ ligand, the dianionic nature of the ligand could stabilize a five-coordinate trigonal bipyramidal Fe(III) ion. Therefore, by simply changing the charges of the ligand, a change in the observed coordination number was achieved.

The change in coordination number of active site metal ions in metalloenzymes is very important during steps involving substrate activation and product release. The mechanism thought to prevail in Mn- and Fe-SODs is thought to involve a change in the coordination number of the active sites. Specifically, the active site in these SODs is thought to undergo a change from five-coordinate in the resting states to six-coordinate in the intermediate states. The deprotonation of the coordinated water and the protonation of the coordinated hydroxide result a change in the active site charge and the subsequent change in coordination number. In this study, we showed that simple deprotonation of the ligating benzimidazole ligand could change the charge of the ligand and result in a change in coordination number.

Acknowledgment. M.S.L. acknowledges the support from the Basic Research Program of the Korea Science & Engineering Foundation (Grant No. R01-2000-000430) and Hanyang University (the program year of 2000). J.S.M. acknowledges the support from the U.S. Department of Energy Division of Materials Science (Grant No. DE FG 03-93ER45504) and the National Science Foundation (Grant No. CHE0110685).

Supporting Information Available: X-ray crystallographic files in CIF format for the structure determination. This material is available free of charge via the Internet at http://pubs.acs.org.

IC011155Q

(18) Lah, M. S.; Chun, H. *Inorg. Chem.* **1997**, *36*, 1782−1785.
(19) (a) Gregorzik, R.; Hartmann, U.; Vahrenkamp, H. *Chem. Ber.* **1994**, *127*, 2117−2122. (b) Hartmann, U.; Gregorzik, R.; Vahrenkamp, H. *Chem. Ber.* **1994**, *127*, 2123−2127.
(20) (a) Noveron, J. C.; Olmstead, M. M.; Mascharak, P. K. *J. Am. Chem. Soc.* **2001**, *123*, 3247−3259. (b) MacBeth, C. E.; Golombek, A. P.; Young, V. G., Jr.; Yang, C.; Kuczera, K.; Hendrich, M. P.; Borovik, A. S. *Science* **2000**, *289*, 938−941. (c) Moliner, N.; Real, J. A.; Muñoz, M. C.; Martínez-Mañez, R.; Juan, J. M. C. *J. Chem. Soc., Dalton Trans.* **1999**, 1375−1380. (d) Ellison, J. J.; Nienstedt, A.; Shoner, S. C.; Barnhart, D.; Cowen, J. A.; Kovacs, J. A. *J. Am. Chem. Soc.* **1998**, *120*, 5691−5700. (e) Daran, J.-C.; Jeannin, Y.; Martin, L. M. *Inorg. Chem.* **1980**, *19*, 2935−2940. (f) Drummond, J.; Wood, J. S. *Chem. Commun.* **1969**, 1373. (g) Ainscough, E. W.; Brodie, A. M.; McLachlan, S. J.; Brown, K. L. *J. Chem. Soc., Dalton Trans.* **1983**, 1385−1389. (h) Davies, J. E.; Gatehouse, B. M. *Acta Crystallogr.* **1972**, *B28*, 3641−3645.